CENTRAL RESEARCH LIBRARY
DOCUMENT COLLECTION

3

ORNL-4312
UC-25 – Metals, Ceramics, and Materials

INTERACTIONS OF REFRACTORY METALS WITH ACTIVE GASES IN VACUA AND INERT GAS ENVIRONMENTS

H. Inouye

OAK RIDGE NATIONAL LABORATORY
CENTRAL RESEARCH LIBRARY
DOCUMENT COLLECTION
LIBRARY LOAN COPY
DO NOT TRANSFER TO ANOTHER PERSON
If you wish someone else to see this document, send in name with document and the library will arrange a loan.

OAK RIDGE NATIONAL LABORATORY
operated by
UNION CARBIDE CORPORATION
for the
U.S. ATOMIC ENERGY COMMISSION

LEGAL NOTICE

This report was prepared as an account of Government sponsored work. Neither the United States, nor the Commission, nor any person acting on behalf of the Commission:

A. Makes any warranty or representation, expressed or implied, with respect to the accuracy, completeness, or usefulness of the information contained in this report, or that the use of any information, apparatus, method, or process disclosed in this report may not infringe privately owned rights; or

B. Assumes any liabilities with respect to the use of, or for damages resulting from the use of any information, apparatus, method, or process disclosed in this report.

As used in the above, "person acting on behalf of the Commission" includes any employee or contractor of the Commission, or employee of such contractor, to the extent that such employee or contractor of the Commission, or employee of such contractor prepares, disseminates, or provides access to, any information pursuant to his employment or contract with the Commission, or his employment with such contractor.

ORNL-4312

Contract No. W-7405-eng-26

METALS AND CERAMICS DIVISION

INTERACTIONS OF REFRACTORY METALS WITH ACTIVE GASES IN VACUA AND INERT GAS ENVIRONMENTS

H. Inouye

OCTOBER 1968

OAK RIDGE NATIONAL LABORATORY
Oak Ridge, Tennessee
operated by
UNION CARBIDE CORPORATION
for the
U.S. ATOMIC ENERGY COMMISSION

CONTENTS

	Page
Abstract	1
Introduction	1
Gas-Metal Equilibria	3
Reaction Kinetics	8
Decarburization	22
Sublimation	24
Interaction of Refractory Metals in Inert Gases	29
Controlling Gas-Metal Reactions	31
Summary and Conclusions	33

INTERACTIONS OF REFRACTORY METALS WITH ACTIVE GASES IN VACUA AND INERT GAS ENVIRONMENTS

H. Inouye

ABSTRACT

The state of our knowledge of the interactions of refractory metals with active gases in vacuum and inert gas environments was reviewed. At temperatures from 600 to 2000°C and at pressures from 10^{-3} to 10^{-10} torr, contamination, degassing, decarburization, and sublimation reactions occur between the refractory metals and absorbed gases.

The extent and kinetics of these reactions are governed by the deviation of the interstitial concentration of the refractory alloy from the equilibrium concentration dictated by the temperature and pressure of the active gas. The reaction rates in inert gases are equivalent to vacua of approximately 10^{-5} to 10^{-7} torr. These interactions can be reduced by minimizing the surface-to-volume ratio of the metal and minimizing the degree of equilibrium disparity. Added control is gained by the use of barrier foil envelopes and the use of low-pressure CH_4 to neutralize the oxidizing gases.

INTRODUCTION

A decade of intensive research and development has shown that refractory alloys based on niobium, molybdenum, tantalum, and tungsten meet many of the requirements of high-temperature service. A remaining technological problem of considerable importance is their interaction with active gases even at low pressures. Use of the high vacuum equipment available has reduced the extent of the gas-metal reactions to levels approaching the limits of detection. In spite of this progress the reactions still occur, for the interstitial content of refractory alloys changes when held at high temperatures.

Because of the limited amounts of active gases available in a vacuum furnace, the reaction rates are correspondingly low and are usually of little consequence for short exposure times; but these low reaction rates extended over a long time could cause interstitial changes

that might significantly affect their properties. The purpose of this study was to determine the nature and the state of knowledge of the interaction of refractory metals with active gases in vacuum and inert gas environments so that methods might be adopted to minimize this universal problem.

A review of the published data shows that the interstitial concentration in refractory alloys changes as a result of contamination, degassing, and decarburization. Because many refractory alloys react with oxygen to form volatile oxides, sublimation is also encountered at the higher temperatures. At temperatures from 600 to 2000°C and at active gas pressures from 10^{-3} to 10^{-10} torr these reactions occur between refractory alloys and gases absorbed on their surfaces — that is, the reactions are characterized by the absence of a surface reaction product.

This paper illustrates by example the principles governing the extent and the kinetics of these processes in terms of the temperature, pressure, reaction time, alloying effects, and specimen geometry. In the first section, we deal with the nature of the environment and consider the contamination and degassing processes in terms of gas-metal equilibria. The second section is a consideration of the reaction kinetics that result from the departure of the interstitial concentration of the refractory metal from the equilibrium value. Decarburization is a special case of the contamination process and is discussed separately in the third section because of its importance to the use of carbide-strengthened alloys. Sublimation, the topic of the fourth section, is considered in this review because it becomes increasingly important in the compatibility of refractory alloys with oxides at the higher temperatures. Because of the lack of sufficient experimental data, the use of inert gases as a substitute for vacuum environments is considered only briefly in the fifth section. In the final section, we suggest methods for controlling the above reactions and describe techniques that reduce the extent of contamination.

Gas-Metal Equilibria

A knowledge of the composition and concentration of the active gases is necessary to understand the high-temperature reactions between refractory metals and their environments. The major impurities in inert gases and in the residual gases in vacuum systems are H_2O, O_2, N_2, CO, CO_2, H_2, and CH_4. These gases originate from system leaks, outgassing of the hot furnace surfaces, the pumping system, and the metal being heated. The pressure of each of these gases is greatly influenced by the history of the hot surfaces and the test conditions. Therefore no specific composition can be assigned to the environment for a given set of conditions.

During the normal heating cycle of the metal in a vacuum, the total pressure of these gases increases to a maximum value, then decreases to a relatively constant low value characteristic of the pumping system. If no attempt is made to regulate the pressure, the interstitial content of the refractory metal will change in the direction of the equilibrium concentration dictated by the temperature and the partial pressures of the various gaseous components.

The extent of the interstitial instability due to nonequilibrium conditions can be determined precisely from the pressure-temperature-composition relationship of the gas pressure is known at a given temperature. As an example, Fig. 1 shows the equilibrium conditions for solutions of nitrogen in niobium.[1] A hypothetical alloy (containing 1 at. % N) is in equilibrium with nitrogen at 5×10^{-4} torr and 1760°C, but at a nitrogen pressure of approximately 1×10^{-5} torr the alloy would degas until the nitrogen content reached 0.16 at. %. At the same temperature but at a nitrogen pressure of 10^{-2} torr, the nitrogen content of niobium would increase eventually to 4 at. %. The nitrogen instabilities arising from temperature fluctuations at a given pressure can be deduced similarly. These data also show that nitrogen will tend to migrate from high to low temperatures in a temperature gradient.

---

[1]J. R. Cost and C. A. Wert, Acta Met. 2, 231-242 (April 1963).

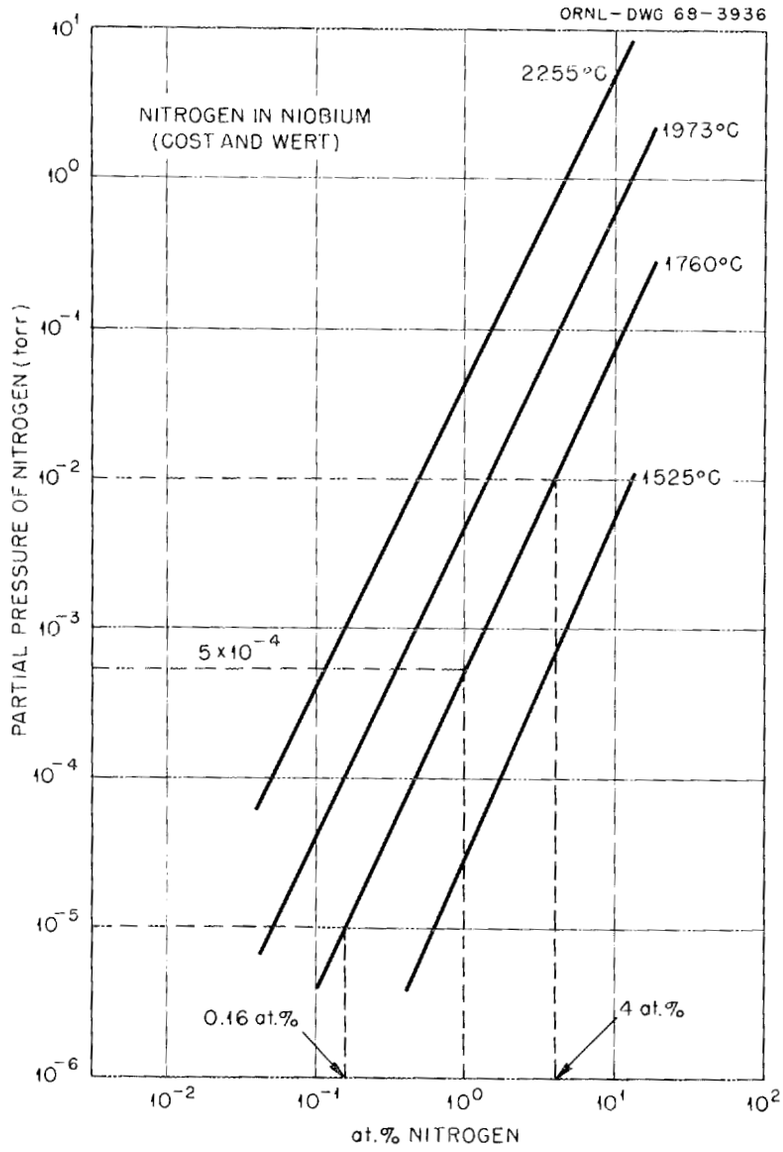

Fig. 1. Isothermal Equilibrium for Niobium-Nitrogen Terminal Solid Solutions.

The precipitation or the solution of interstitial phases is a form of interstitial instability that has an important effect on the mechanical properties of refractory alloys. Gas-metal equilibria such as that shown in Fig. 2 precisely define the conditions of stability of the Ta_2N precipitated phase.[2] Note, however, that in this case the

[2] E. Gebhardt *et al.*, *Z. Metallk.* *52*, 464–473 (1961).

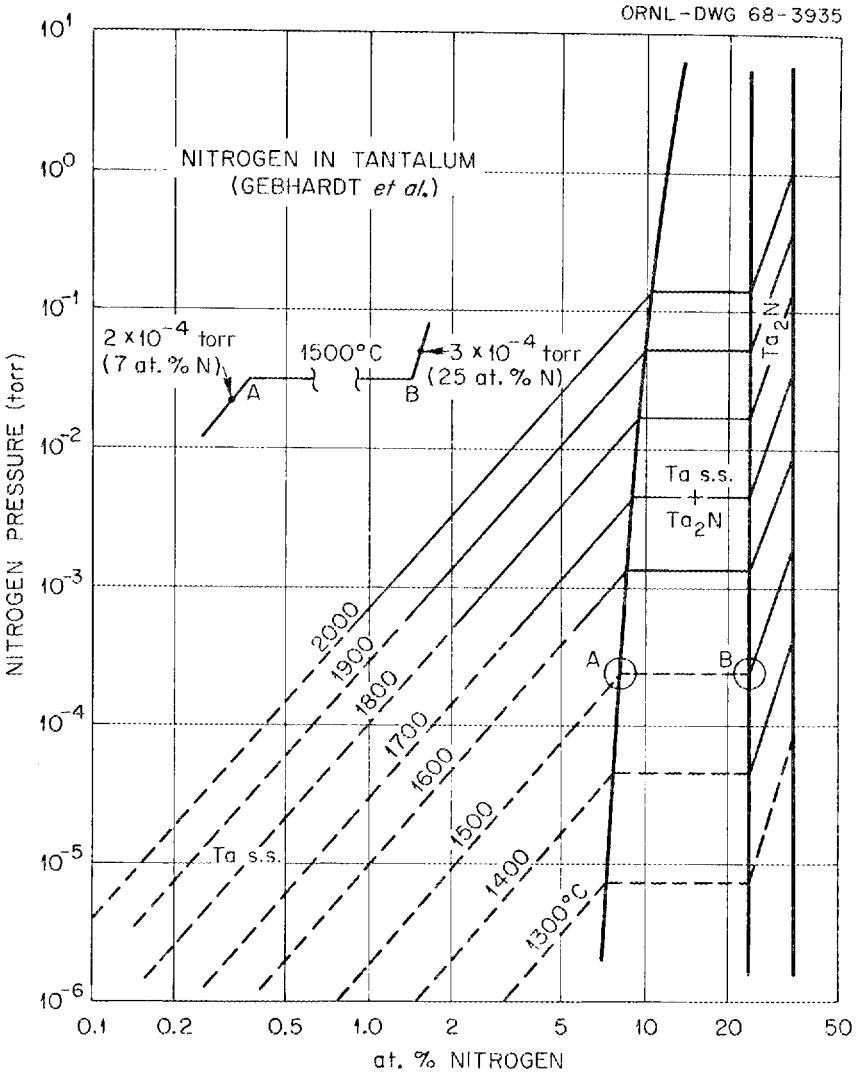

Fig. 2. Pressure Composition Relationships at Equilibrium for the Tantalum-Nitrogen System from 1300 to 2000°C.

nitrogen pressures over the tantalum-nitrogen alloys in the two-phase regions are constant. The difficulty in controlling the quantity of Ta_2N phase at a given temperature can be illustrated by determining the equilibrium nitrogen pressures of the circled points at A and B at 1500°C. These points on the diagram are shown by the arrows in the upper left corner of Fig. 2. A hypothetical alloy containing Ta_2N would not dissolve nor increase in quantity so long as the nitrogen pressure was equal to the decomposition pressure of the nitride (estimated to be approximately 2.5×10^{-4} torr). If the nitrogen pressure

were 2.0×10^{-4} torr as in point A, the nitrogen content would decrease to 7 at. % N, and the Ta_2N would go into solution; at a pressure of 3×10^{-4} torr, the nitrogen content would increase to 25 at. % N, and the alloy eventually would be converted to Ta_2N.

The affinity of refractory metals for gases and their solubility in them are altered markedly by alloying elements, as Table 1 (ref. 3) indicates. These data show that oxygen solubility in niobium is lowered from 0.5 wt % at 1000°C to about 0.2 wt % by magnesium and is in the range 0.01 to 0.02 wt % in the presence of calcium. On the other hand, the affinity of niobium for oxygen is increased markedly by these elements. These data further show that niobium containing 100 ppm O would be contaminated by most oxides with oxygen. The alloying components — zirconium, titanium, and hafnium — present in many of the current alloys are also expected to lower the oxygen solubility since their free energies of formation are also high.

Table 1. Changes of the Thermodynamic Potentials Associated with the Formation of Nb-O Solutions at 1000°C[a]

Phase in Equilibrium with Nb-O Solution	Oxygen in Solution, wt %	$-\Delta F°$ (1273°K) (kcal/mole O_2)
CaO	0.01–0.02	242
MgO	~ 0.20	224
NbO	~ 0.50	168

[a]G. A. Meerson and T. Segorcheanu, Affinity of Niobium for Oxygen, USAEC Translation AEC-tr-5910 (Aug. 22, 1963).

Whereas the solubility limit of oxygen in niobium is lowered by zirconium,[4] the nitrogen solubility limit is increased from 0.43 wt %

[3]G. A. Meerson and T. Segorcheanu, Affinity of Niobium for Oxygen, USAEC Translation AEC-tr-5910 (Aug. 22, 1963).

[4]D. O. Hobson, "Aging Phenomena in Columbium-Base Alloys," pp. 325–334 in High Temperature Materials, Vol II, Interscience, New York, 1963.

in niobium[5] to approximately 0.75 wt % in Nb–0.86 wt % Zr at 1400°C.[6] The solution characteristics of nitrogen in unalloyed niobium and in Nb–1% Zr are significantly different, as Fig. 3 (refs. 7,8) shows. These data show that 1 wt % Zr lowers the equilibrium nitrogen pressure over the alloy at given nitrogen concentrations.

---

[5]W. M. Albrecht and W. D. Goode, Jr., Reaction of Nitrogen with Niobium, BMI-1360 (July 1959).

[6]E. de Lamotte et al., Equilibrium Solutions of Nitrogen in Columbium Base Alloys, Air Force Materials Laboratory, Report No. ML-TDR-64-134, Technical Documentary Report (June 1964).

[7]R. A. Pasternak et al., J. Electrochem. Soc. 113(7), 731–735 (1966).

[8]H. Inouye, Equilibrium Solid Solutions of Nitrogen in Nb–1% Zr Between 1200 to 1800°C, ORNL-TM-1355 (February 1966).

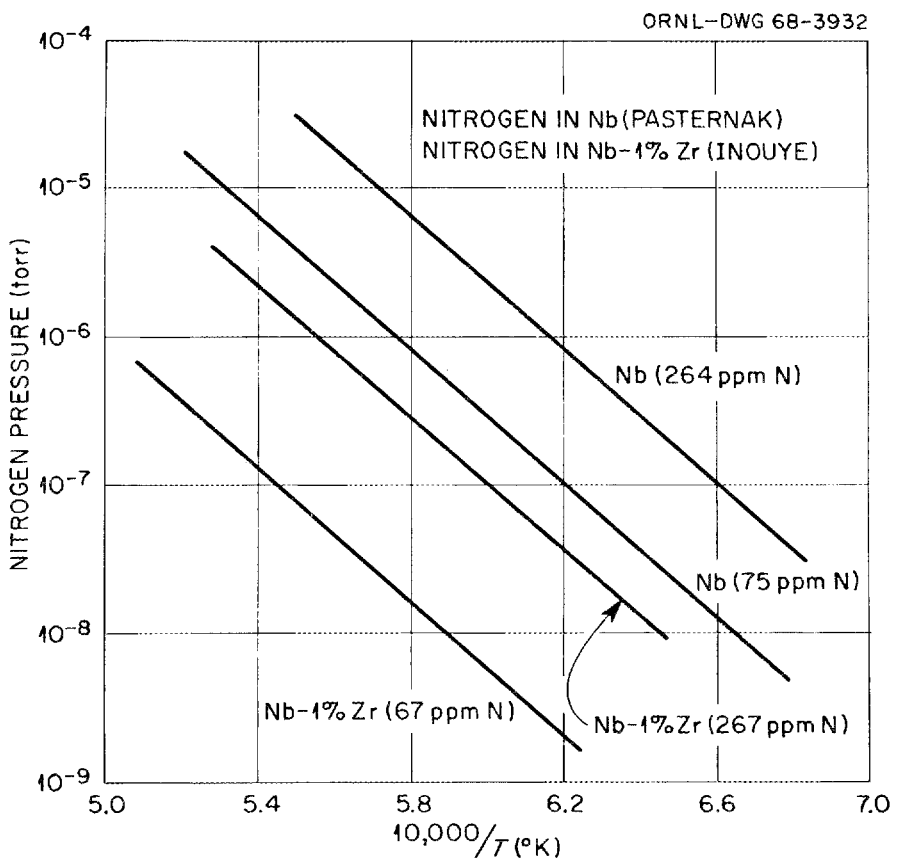

Fig. 3. Comparison of the Solution Equilibrium of Nitrogen in Niobium with Nitrogen in Nb–1% Zr.

It is estimated that zirconium increases the concentration of nitrogen in solution by a factor of about 4 (> 267/75) at a given temperature and pressure. The oxides and nitrides of molybdenum and tungsten have a lower free energy of formation than oxides and nitrides of niobium and tantalum. Therefore, the interactions of molybdenum and tungsten with oxygen and nitrogen are expected to be less extensive than those of the latter metals. Molybdenum and tungsten alloyed with active alloying elements such as titanium, zirconium, and/or hafnium, however, are expected to be as reactive toward the above gases as are the alloys of niobium and tantalum containing these elements.

Reaction Kinetics

As discussed in the previous section, the conditions of equilibrium between a gas and the interstitial concentration in a metal are defined precisely. Since this state is rarely attained under a normal heating cycle, it follows that the interstitial concentration will tend to change as required by thermodynamic equilibrium. The rate of this change and the parameters that control the extent are covered in this section.

The factors governing the reaction kinetics between low-pressure gases and metal surfaces that result in contamination can be deduced from a model based on the kinetic theory of gases. For example, the mass incident rate, Q_i, of a gas at a surface in a vacuum is given by $5.833 \times 10^{-2}\ P\sqrt{M/T}$. Let it be assumed that a gas molecule in a vacuum system incident on the metal surface is either absorbed or rebounds. The rate of the surface reaction is then given by

$$Q_a = \alpha Q_i = \alpha[5.833 \times 10^{-2}\ P(MT^{-1})^{\frac{1}{2}}] \ , \qquad (1)$$

where

Q_a = absorption rate, g cm^{-2} sec^{-1},
Q_i = incident rate, g cm^{-2} sec^{-1},
P = gas pressure, torr,
M = molecular weight of the gas, g, and
T = absolute temperature, °K.

The parameter, α, is dimensionless and is the probability that the impinging gas will become absorbed; hence this parameter is called the sticking probability. Since the pressure in the vacuum system is P_o when measured at an ambient temperature of T_o (°K), its pressure at T is greater by the temperature ratio $(T/T_o)^{\frac{1}{2}}$; that is, $P = P_o(T/T_o)^{\frac{1}{2}}$. Substituting this pressure correction due to thermal transpiration in Eq. (1) gives

$$Q_a = \alpha[5.833 \times 10^{-2}\ P_o(MT_o^{-1})^{\frac{1}{2}}] \ . \tag{2}$$

Let it be further assumed that the absorbed gas diffuses into the interior of the metal of surface area A (cm^2) and weight W (g). The change in concentration, ΔC_m(g of gas/g of metal) of the interstitial in the alloy for a reaction time, Δt (sec) is then

$$\Delta C_m = Q_a\ \Delta t\ A/W \ . \tag{3}$$

Since A/W is equal to $A/\rho V$ and A/V is equal to 1/X, Eq. (3) can also be expressed by

$$\Delta C_m = Q_a\ \Delta t\ A/\rho V \ , \tag{4}$$

or

$$\Delta C_m = Q_a\ \Delta t/\rho X \ , \tag{5}$$

where

ρ = density of the metal, g/cm^3,

V = volume of metal exposed to the gas, cm^3, and

X = thickness of metal exposed to the gas, cm.

Equations (1) and (2) state that the contamination rate of a metal by a gas is proportional to the sticking probability and the test pressure. Further, the extent of the contamination [Eqs. (3–5)] is shown to be proportional to the reaction time and surface-to-volume ratio and inversely proportional to the thickness. The derived expressions do not include the effect of temperature, which is known

to be an important variable, because the incident rate of the gas is independent of the temperature as Eq. (2) shows. Thus, although the sorption expressions do not explicitly show the effect of temperature, it is evident that this variable must influence the value of α, which ranges between 0 and 1.

Equations (4) and (5) illustrate the relationship between the extent of contamination and the geometry of the metal, an important factor frequently overlooked by those concerned with contamination control. Experimental verification of the geometry effects predicted by these two expressions is contained in the data tabulated in Tables 2 and 3. Table 2 shows that the oxygen contamination of tantalum[9] was greater for the 0.010- than the 0.020-in.-thick specimens. Note that the results for nitrogen contamination after about 13 hr do not agree with the predictions. This we believe to be due to the attainment of equilibrium between the nitrogen in the argon and in the metal, in which case the geometry effects stated in Eqs. (4) and (5) are invalid. The data in Table 3 show more clearly the effects of the specimen thickness of Nb-1% Zr on the extent of contamination.[10] In this case the geometry effects of the specimen on contamination are compared for the same conditions of environment and reaction time. As in the previous example, the extent of contamination is greater in the thinner specimens than in the thicker specimens at temperatures from approximately 850 to 1200°C. The last column in Table 3 shows that $\Delta C_1/\Delta C_2 = X_2/X_1$, a relationship that can be obtained from Eq. (5) for specimens of different thicknesses.

In light of the various derived expressions above, the kinetics of the contamination process are seen to depend on the value of α, which is the dimensionless parameter defined in Eqs. (1) and (2) as the sticking probability and which is equal to the ratio of Q_a/Q_i. Typically the values of α are low at high temperatures and do not vary uniformly

---

[9] High Temperature Materials Program Report, GEMP-25A, No. 25 (July 1963).

[10] H. Inouye, "The Contamination of Refractory Metals in Vacua Below 10^{-6} Torr," pp. 871-883 in Refractory Metals and Alloys III: Applied Aspects, Vol 30, ed. by Robert I. Jaffee, Gordon & Breach Science Publishers, New York, 1966.

Table 2. Contamination of Tantalum Stress-Rupture Specimens in Argon at 2600°C[a]

Time at Temperature (hr)	Specimen Thickness 0.010 in.		Specimen Thickness 0.020 in.	
	ΔO	ΔN	ΔO	ΔN
1.05	498	84		
3.45	399	78		
12.67	266	276		
1.10			131	87
7.58			178	154
13.60			187	259

[a]High Temperature Materials Program Report, GEMP-25A, No. 25 (July 1963).

Table 3. The Effect of Specimen Thickness on the Contamination of Nb–1% Zr[a]

Test Temperature (°C)	Specimen Thickness, in.		Contamination[b] ppm (wt)		Ratio	
	X_1	X_2	ΔC_1	ΔC_2	X_2/X_1	$\Delta C_1/\Delta C_2$
856	0.0201	0.0391	724	378	1.94	1.91
988	0.0200	0.0308	966	646	1.54	1.50
1081	0.0200	0.0384	1396	696	1.92	2.01
1135	0.0198	0.0393	1506	766	1.98	1.97
1201	0.0197	0.0382	2464	1354	1.94	1.72

[a]H. Inouye, "The Contamination of Refractory Metals in Vacua Below 10^{-6} Torr," pp. 871–883 in Refractory Metals and Alloys III: Applied Aspects, Vol 30, ed. by Robert I. Jaffee, Gordon & Breach Science Publishers, New York, 1966.

[b]Sum of oxygen, carbon and nitrogen contamination at an average pressure of 5.6×10^{-7} torr over 984 hr.

with temperature. As an example, the initial reaction rate between Nb–1% Zr (initially containing 51 ppm N) and nitrogen expressed in terms of α between 800 and 1600°C is shown in Fig. 4 (ref. 11). At 800°C the values of α are about 0.07 and decrease slowly to minima of about 0.05 at 1125°C. Above 1125°C, α increases to a maximum value of approximately 0.09, depending on the pressure, then decreases rapidly to zero at the highest temperatures. For the test conditions shown, the maximum value of α was less than 0.10 – that is, less than 10% of the incident nitrogen was sorbed by Nb–1% Zr. Another example is

[11]H. Inouye, "High-Temperature Sorption of Nitrogen by Nb–1% Zr in Ultrahigh Vacuum," to be submitted for publication.

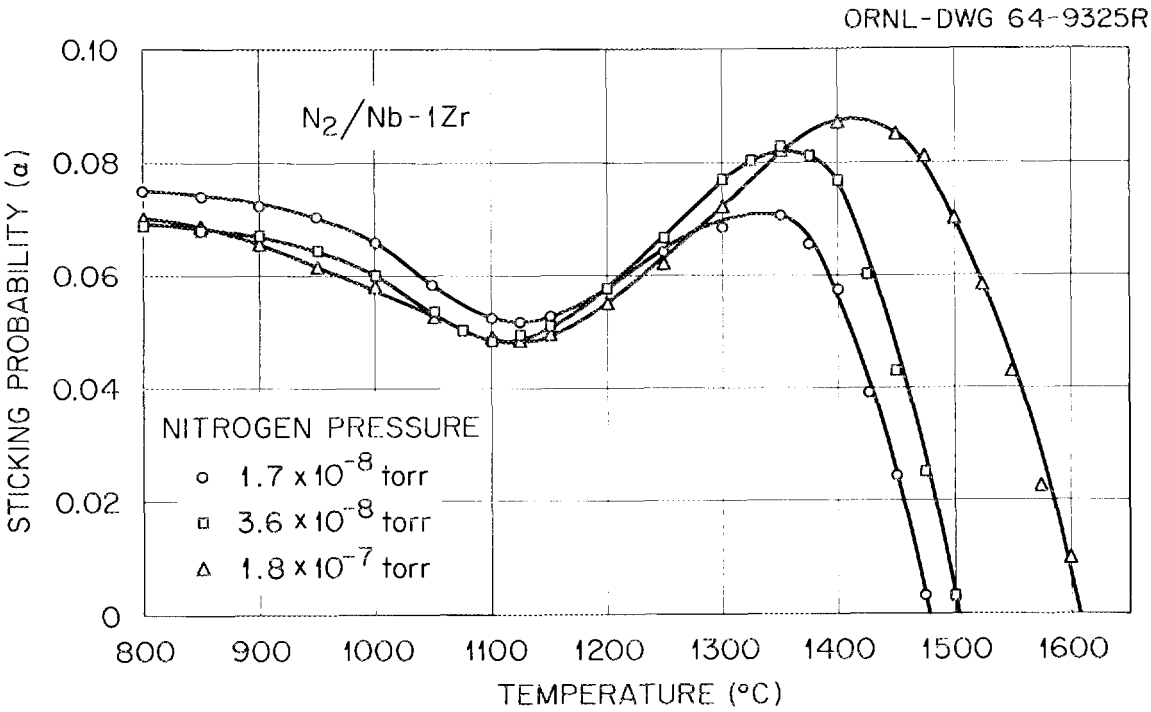

Fig. 4. Variation of the Sticking Probability Versus Temperature for the Reaction of Nitrogen with Nb–1% Zr for Pressures from 10^{-8} to 10^{-7} torr. Reaction time, 10 min; initial nitrogen concentration, 51 ppm.

shown in Fig. 5. In this case a maximum of about 4% of the incident oxygen reacts with tungsten[12] and, like the nitrogen reaction with Nb–1% Zr, α shows both minima and maxima.

The intersections of the separate curves with the abscissa at $\alpha = 0$ in Fig. 4 correspond to the equilibrium temperatures and pressures for Nb–1% Zr containing 51 ppm N (see Fig. 6). Since the equilibrium conditions change with the nitrogen content of the alloy, α would be zero at other temperatures and pressures as the nitrogen content varied. Variations in the initial nitrogen content also influence the values of α for this alloy, as shown below:

Initial Nitrogen Content of Nb–1% Zr, ppm	α at 1200°C
10	0.089
11	0.071
51	0.057
67	0.052
90	0.038

Thus, Fig. 4 and these data show that α is dependent on the interstitial content of the alloy, the temperature, and the pressure of the gas. Therefore, the curves shown in Fig. 4 would shift to the left and downward if the nitrogen content were higher and to the right and upward if the nitrogen content were lower.

With the continued sorption of nitrogen over an extended period of time, α continuously decreases, as would be expected from the data tabulated above. The manner by which α varies with the concentration is illustrated in Fig. 7. These data represent the kinetics of the reaction when the absorbed nitrogen remains in solution. The later stages of sorption are represented by straight lines whose equation is

$$\alpha = \alpha_o(1 - C_m/C_e) \ , \qquad (6)$$

[12] J. H. Singleton, J. Chem Phys. 45(8), 2819–2826 (1966).

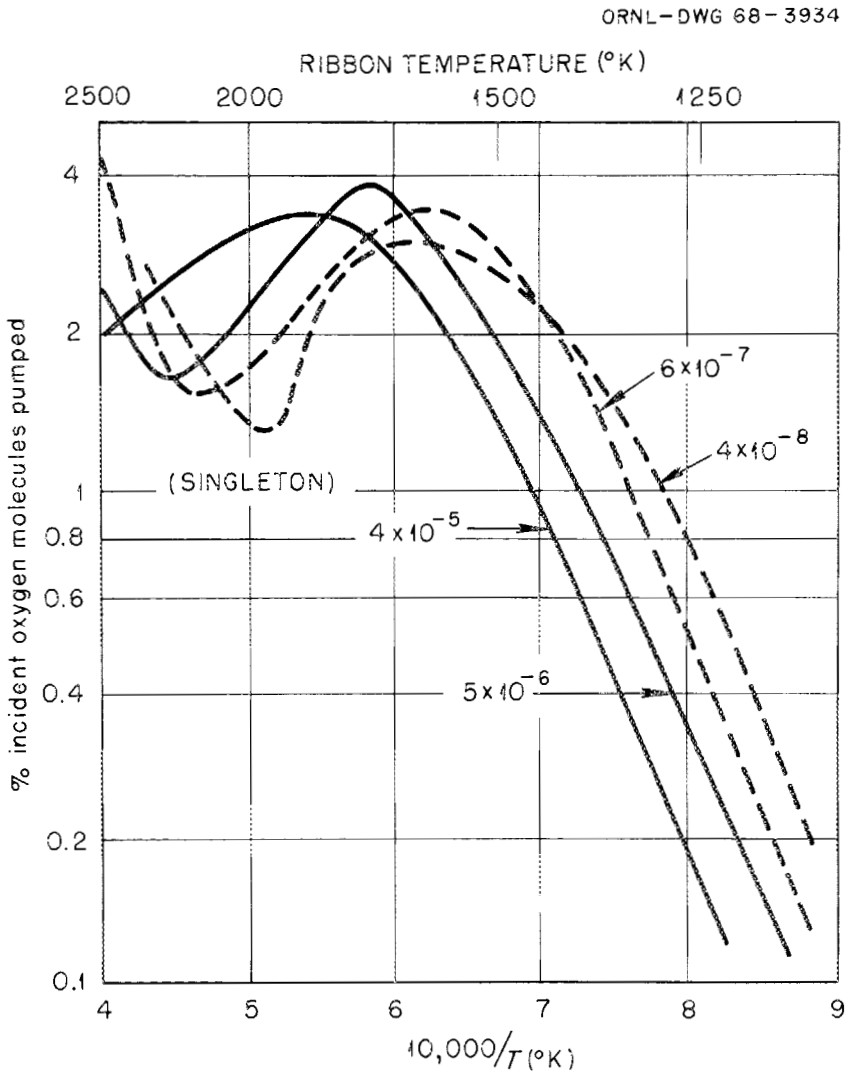

Fig. 5. Variation of the Sticking Probability Versus Temperature for the Reaction of Oxygen with Tungsten. Initial P_{O_2} (torr) before heating tungsten is indicated for each curve.

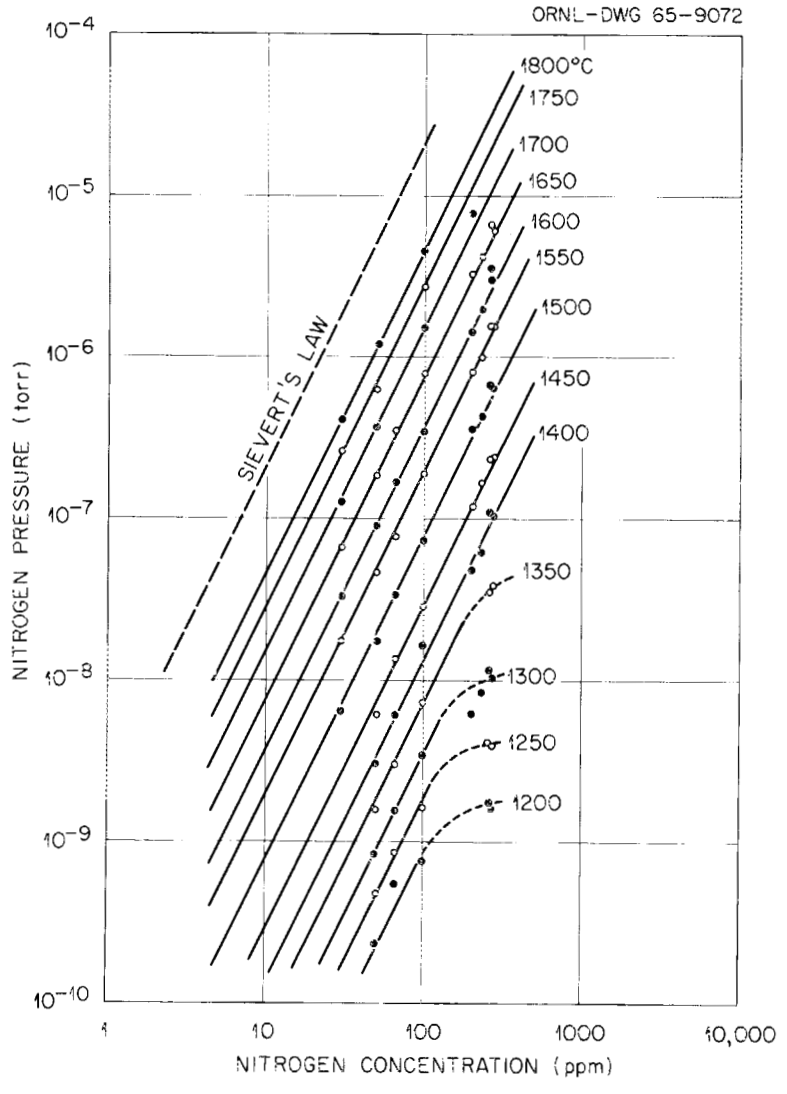

Fig. 6. Pressure-Composition Relationship at Equilibrium for Solutions of Nitrogen in Nb–1% Zr from 1200 to 1800°C.

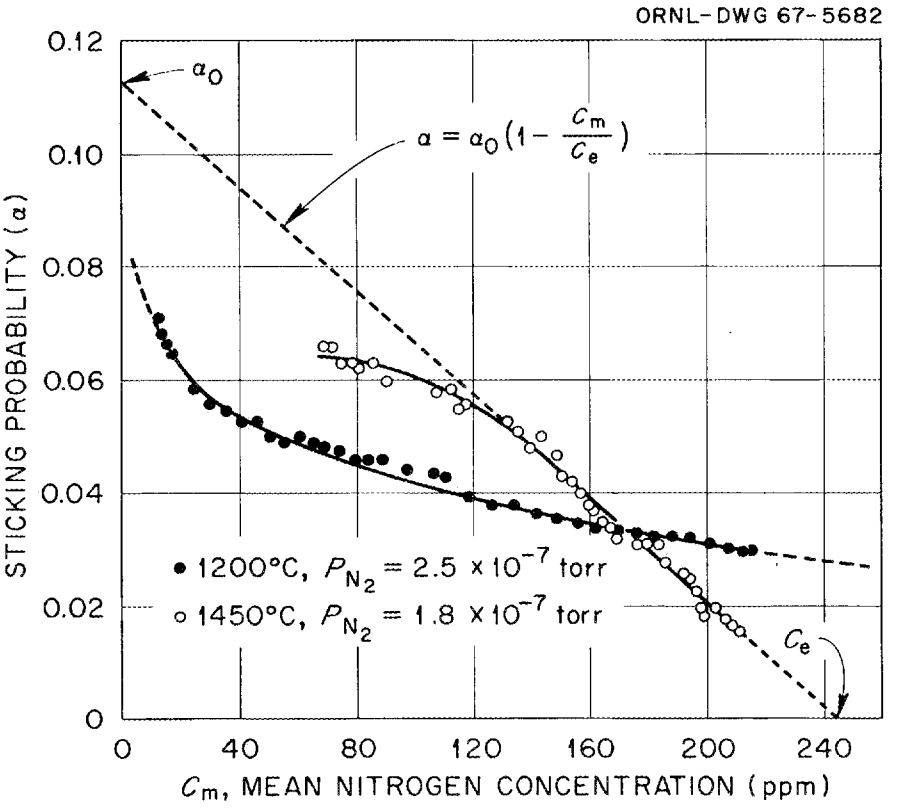

Fig. 7. Relationship Between Sticking Probability and the Mean Nitrogen Concentration of Nb–1% Zr at a Nitrogen Pressure of 2.5×10^{-7} torr and 1200°C and at a Nitrogen Pressure of 1.8×10^{-7} torr at 1450°C.

where

α_0 = sticking probability for a hypothetical nitrogen-free alloy,

C_m = mean nitrogen concentration in solution, ppm, and

C_e = equilibrium nitrogen concentration, ppm.

The ratio C_m/C_e corresponds to the fractional saturation of the alloy with nitrogen, and the quantity $(1 - C_m/C_e)$ corresponds to the deviation from equilibrium. Therefore the reaction rate of a gas with a metal whose surface is free of a reaction product is seen to be proportional to the "equilibrium disparity" – that is, the deviation of the instantaneous interstitial concentration from the interstitial concentration the alloy would contain at equilibrium.

When the sorption process is continued so that the interstitial concentration in the alloy exceeds the solubility limit, the kinetics are altered as shown in Fig. 8. These data show that the value of α for the reaction between niobium and nitrogen decreases continuously with C_m as in Fig. 7; at the solubility limit, however, the smooth curve exhibits a kink as α becomes constant[13] because the concentration of nitrogen in solution, C_m, remains constant due to the precipitation of Nb_2N. When this condition is attained, the quantity $(1 - C_m/C_e)$ in Eq. (6) becomes constant and therefore accounts for the constancy of α beyond the solubility limit.

Since it has been determined that the value of α is governed by the "equilibrium disparity" of the interstitial in solution, the experimental data which follow can now be explained. For example, Eq. (1) predicts that the reaction rate of a gas with a metal will increase linearly with the test pressure. This relationship is experimentally verified by the data of Fig. 9 for the reaction of nitrogen with Nb–1% Zr in runs of 10 min (ref. 14). Similar results are obtained for the reaction of oxygen with Nb–1% Zr, as Fig. 10 (ref. 15) shows. The reason for the linear relationship between the reaction rate and the test pressure in Fig. 9 is that the change in C_m for a reaction time of 10 min under these conditions of temperature and pressure varies from 2.8×10^{-4} to 0.77 ppm for the geometry of the sample tested and therefore has no significant effect on the quantity $(1 - C_m/C_e)$ in Eq. (6). The linear relationship between the reaction rate and pressure, seen in Fig. 10, is obeyed for a different reason. In this case we believe that, due to the low oxygen solubility in Nb–1% Zr, zirconium oxide is being precipitated

---

[13]R. A. Pasternak et al., J. Electrochem. Soc. 113(7), 731–735 (1966).

[14]H. Inouye, "High-Temperature Sorption of Nitrogen by Nb–1% Zr in Ultrahigh Vacuum," to be submitted for publication.

[15]L. Rosenblum et al., Oxidation of Columbium, Tantalum, and Their Alloys, NASA-SP-131, pp. 170–187 (Aug. 23–24, 1966).

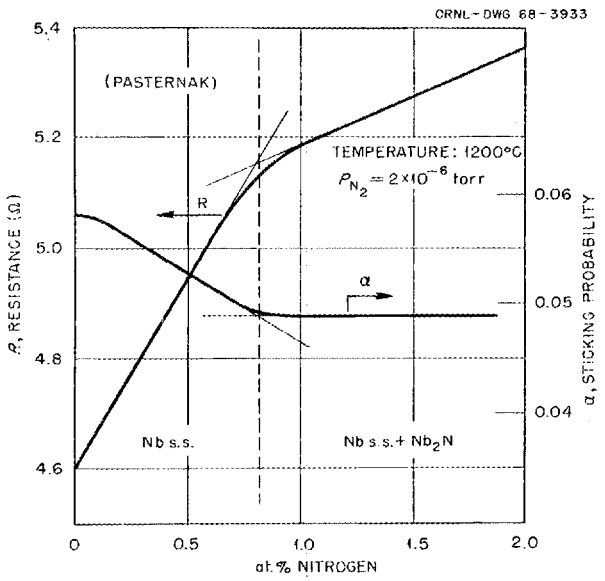

Fig. 8. The Resistivity and Sticking Probability as a Function of the Nitrogen Concentration for the Reaction of Niobium with Nitrogen at 1200°C.

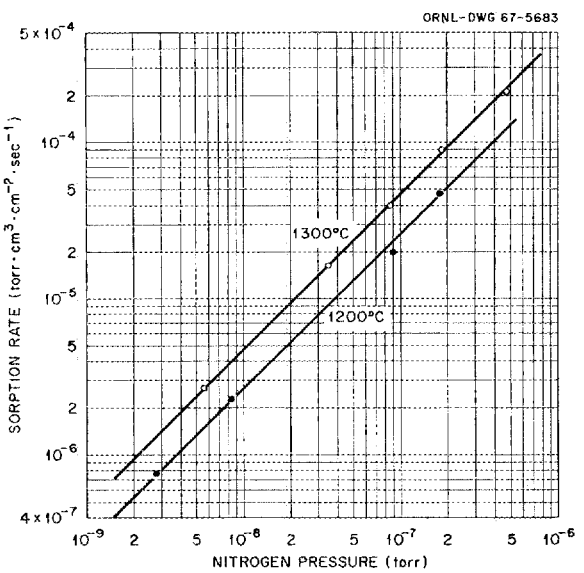

Fig. 9. Relationship Between Sorption Rate of Nitrogen by Nb–1% Zr and the Nitrogen Pressure at 1200 and 1300°C.

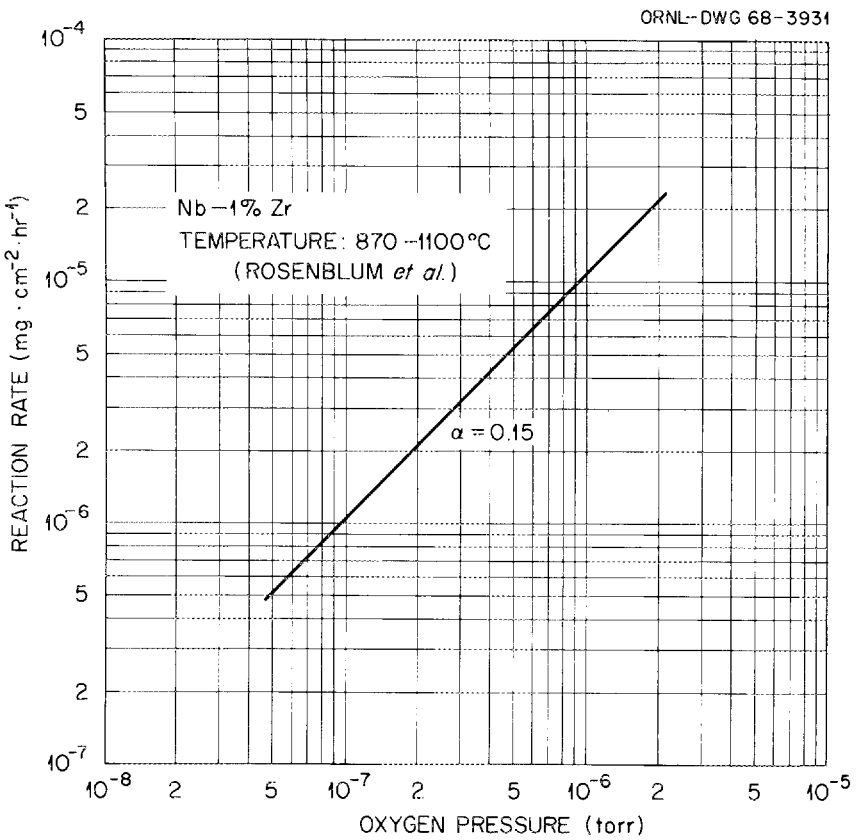

Fig. 10. Oxidation Rate of Nb–1% Zr as a Function of the Oxygen Pressure from 870 to 1100°C.

within the alloy at a rate equal to the rate of oxygen uptake. Since the matrix is saturated with oxygen at a constant concentration, C_m, and since C_e is fixed by the temperature and pressure, the factor $(1 - C_m/C_e)$, which governs the reaction rate, is also constant. This result is analogous to the example shown in Fig. 8.

The occurrence of the maxima in the values of α at the intermediate temperatures of approximately 1300°C shown in Fig. 4 can also be explained in terms of Eq. (6). Since the quantity $(1 - C_m/C_e)$ was determined to be constant for reaction times of 10 min, α_o therefore must increase with temperature. Above the maxima, α is influenced principally by C_e, whose value at a given pressure decreases with increasing temperature as required by the equilibrium relationships in Fig. 6. Thus, when C_m is not significantly less than C_e, small increases

in temperature rapidly cause the ratio C_m/C_e to approach unity, and α therefore correspondingly decreases.

The reaction rates of a gas with a metal over an extended period of time can also be deduced from Eq. (6). At a given temperature and pressure, C_m will increase continuously with the reaction time until its value ultimately equals C_e. When the sorption process results in the solution of the interstitial, Q_a will decrease since α decreases; and, as may be seen from Eq. (3), ΔC_m would not be expected to increase linearly with the reaction time as experimentally verified by the data shown in Fig. 11. In contrast, when the pressure and temperature conditions favor the formation of an interstitial compound, C_m will remain constant at the solubility limit. Figure 12 shows the expected linear relationship between the weight gain of Nb–1% Zr in oxygen as a function of time[16] due to the low oxygen solubility in the alloy.

---

[16]T. K. Roche, "Effect of Degree of Vacuum on the Slow-Bend Creep Behavior of Columbium–0.6% Zirconium at 1000°C," pp. 901–916 in Refractory Metals and Alloys III: Applied Aspects, Vol 30, ed. by Robert I. Jaffee, Gordon & Breach Science Publishers, New York, 1966.

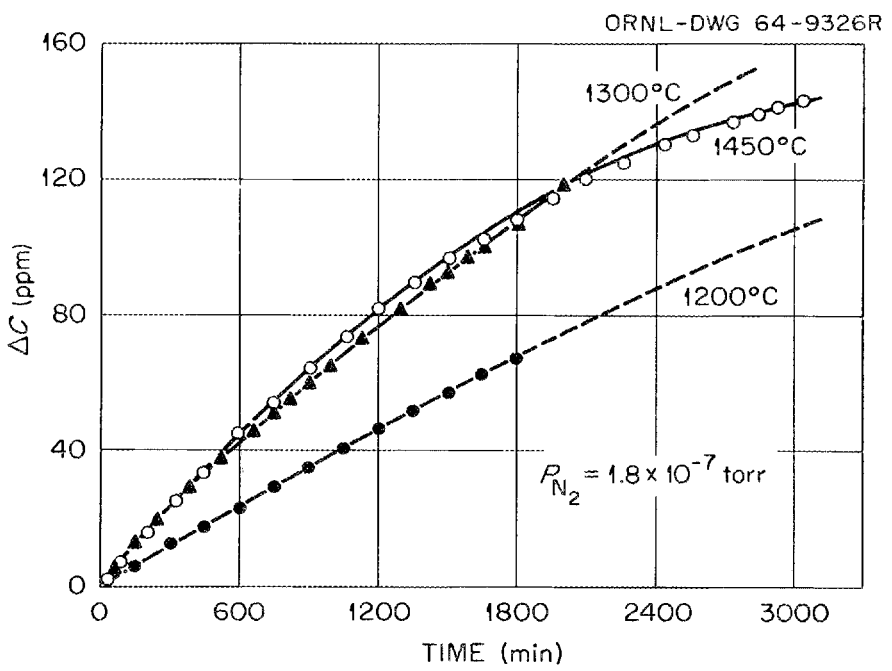

Fig. 11. The Increase in Nitrogen Content of Nb–1% Zr at a Nitrogen Pressure of 1.1×10^{-7} torr and Temperatures of 1200, 1300, and 1450°C.

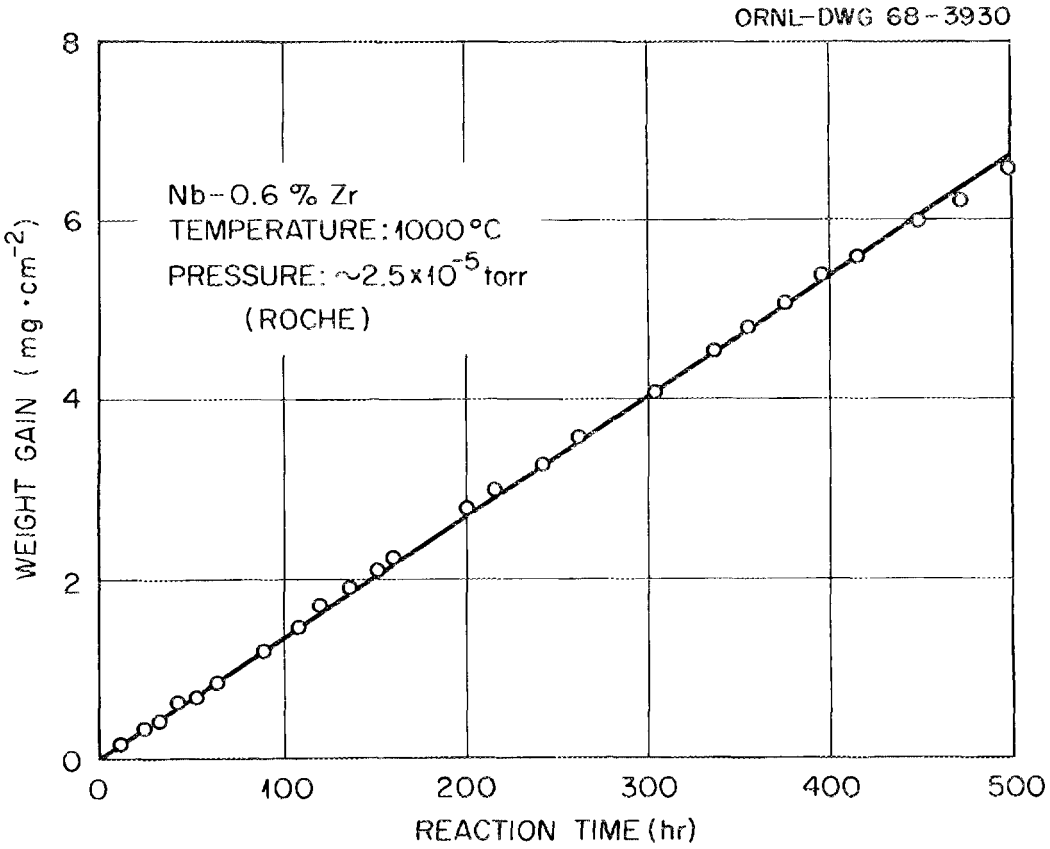

Fig. 12. Weight Gain of Nb–0.6% Zr as a Function of Time at a Pressure of 2.5×10^{-5} torr and a Temperature of 1000°C.

The expected effects of alloying elements on the reactivity of refractory metals with gases can be deduced from the above examples. If the alloying element lowers the solubility limit, it is more probable that the gas-metal interaction for a given temperature and pressure condition will result in the precipitation of a second phase. Figures 8 and 12 show that when these conditions prevail the reaction rates remain constant; and over a long reaction period, it would be expected that the alloy would be contaminated to a greater extent than the pure metal. Moreover, alloying elements that lower the solubility limit increase the thermodynamic potential of the interstitial in the alloy, as illustrated in Table 1, and therefore would likely increase the reaction rates. On this basis, zirconium, titanium, and hafnium, which are the principal constituents in many of our current alloys, would be expected to increase the reactivity of the base alloy toward oxygen. Table 4

compares the oxygen contamination of unalloyed molybdenum, niobium, and tantalum with the corresponding alloys containing the reactive elements titanium, zirconium, and hafnium. In each case, these data confirm the alloying effects postulated above.

Table 4. Effect of Alloying Elements on the Oxygen Contamination of Molybdenum, Niobium, and Tantalum at 1200°C[a]

Alloy Designation	Alloying Element(s) (wt %)	Alloy Base	Oxygen Contamination,[b] ppm	
			Alloy	Base
TZM	0.5 Ti + 0.08 Zr	Mo	340	−9
FS-80	1 Zr	Nb	320	100
T-111	2 Hf + 8 W	Ta	180	29

[a]H. Inouye, "The Contamination of Refractory Metals in Vacua Below 10^{-6} Torr," pp. 871–883 in Refractory Metals and Alloys III: Applied Aspects, Vol 30, ed. by Robert I. Jaffee, Gordon & Breach Science Publishers, New York, 1966.

[b]1000 hr at 2.5×10^{-7} torr.

It is obvious that there are test conditions that could also cause degassing of the interstitial. According to Eq. (6) degassing would occur when $C_m > C_e$, and negative values of α would be obtained. An example of the reversibility of the nitrogen reaction with niobium[17] is given by Fig. 13. In this experiment nitrogen was allowed to react with niobium at 2×10^{-6} torr at 1367°C almost to saturation. The reaction rate expressed in terms of α decreased as in segment (a). When the nitrogen pressure was increased to 4×10^{-6} torr, additional nitrogen reacted with niobium as in (b); then, when the nitrogen pressure was decreased to the initial pressure of 2×10^{-6} torr, the sample degassed as in segment (c).

[17]R. A. Pasternak et al., J. Electrochem. Soc. 113(7), 731–735 (1966).

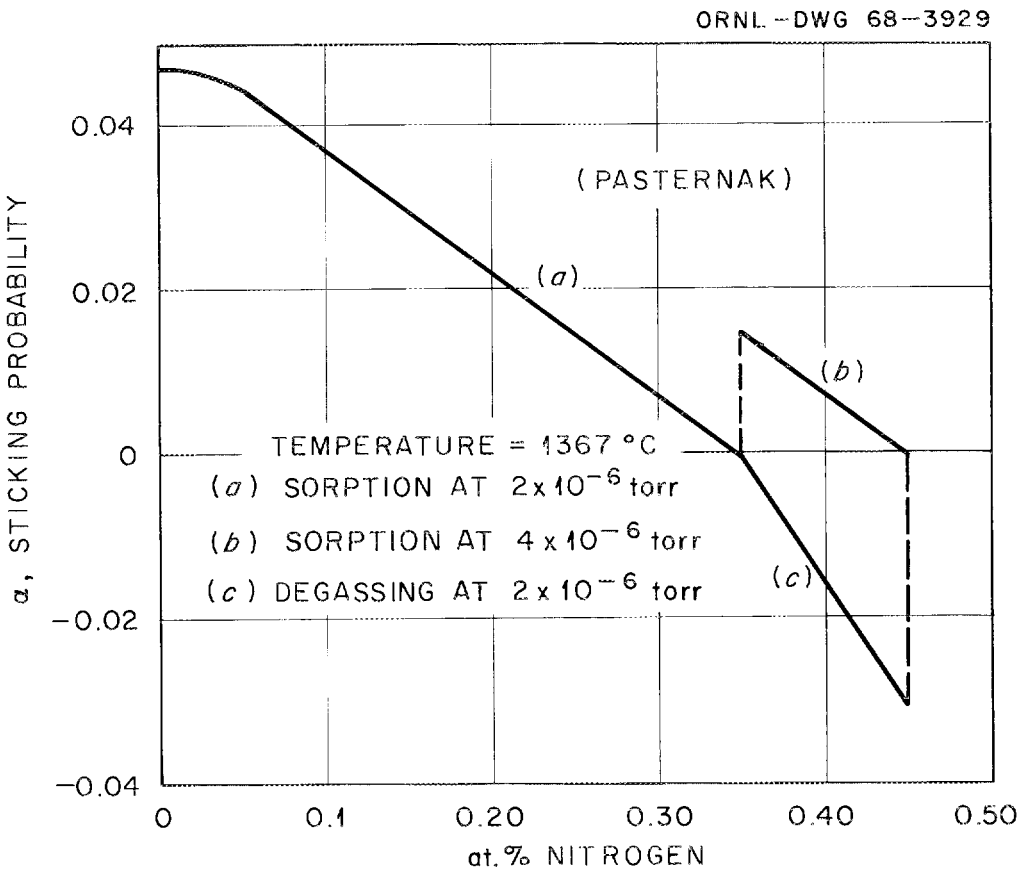

Fig. 13. Sticking Probability as a Function of Nitrogen Content for the Reaction of Nitrogen with Niobium at 1367°C.

Decarburization

All refractory alloys contain carbon as an impurity, and several contain up to 0.1 wt % as an intentional alloying component to enhance their strength through the formation of carbides. Although the carbon concentration can be controlled within small variations in the fabricated state, this element can be most difficult to maintain at the desired level at high temperatures if the environment is not under control. A principal variable affecting carbon stability according to Table 5 is the test pressure.[18] For the examples given, decarburization occurred under all test conditions and was most severe at the

[18]D. T. Bourgette, Trans. Vacuum Met. Conf., 8th, New York, 1965, 57–73 (1966).

Table 5. Effect of Pressure and Temperature on the Stability of Interstitials in Refractory Alloys[a]

Alloy Designation	Temperature (°C)	Pressure (torr)	Change in Interstitial Concentration, ppm[b]			
			Carbon	Oxygen	Nitrogen	Hydrogen
D-43	1500	2×10^{-9}	−50	−16	−56	−3
	1500	2×10^{-8}	−50	−13	−66	−3
	1500	1.5×10^{-7}	−400	+101	+351	−3
	1300	1×10^{-9}	−20	−12	−63	−4
	1300	5×10^{-7}	−380	+347	+244	−4
FS-80	1500	3×10^{-9}	−70	−175	−53	−6
	1500	6×10^{-7}	−97	0	+92	−6
	1300	5×10^{-9}	−10	−137	−32	−7
	1300	5×10^{-7}	−48	−40	+6	−4
T-111	1500	2×10^{-9}	−10	−56	−8	−3
	1500	5×10^{-7}	−30	+40	+171	−3

[a]D. T. Bourgette, Trans. Vacuum Met. Conf. 8th, New York, 1965, 57–73 (1966).

[b]500- to 750-hr tests.

higher test pressures of approximately 10^{-7} torr. Note from the tabulated data that the large carbon losses at 10^{-7} torr are accompanied by a corresponding increase in the oxygen and nitrogen contents. Posttest chemical analyses showed that the carbon and the oxygen contents of the alloys expressed as a carbon-to-oxygen ratio was a function of pressure (Fig. 14) and temperature (Fig. 15). Note in Fig. 14 that D-43 with an initial carbon-to-oxygen ratio of 15.5 will decarburize at 1500°C when the pressure in the vacuum system exceeds 1×10^{-8} torr; Fig. 15 shows that the carbon-oxygen interaction in Nb–1% Zr, which increases with temperature, becomes a significant factor above 1200°C (ref. 18). These correlations suggest that decarburization is due to the formation of carbon monoxide that is removed from the furnace by the vacuum pumps.

A carbon-oxygen interaction has been established to be a mechanism for the decarburization of tungsten by Becker *et al.*[19] who studied

[19]J. A. Becker *et al.*, J. Appl. Phys. 32(3), 411–423 (March 1961).

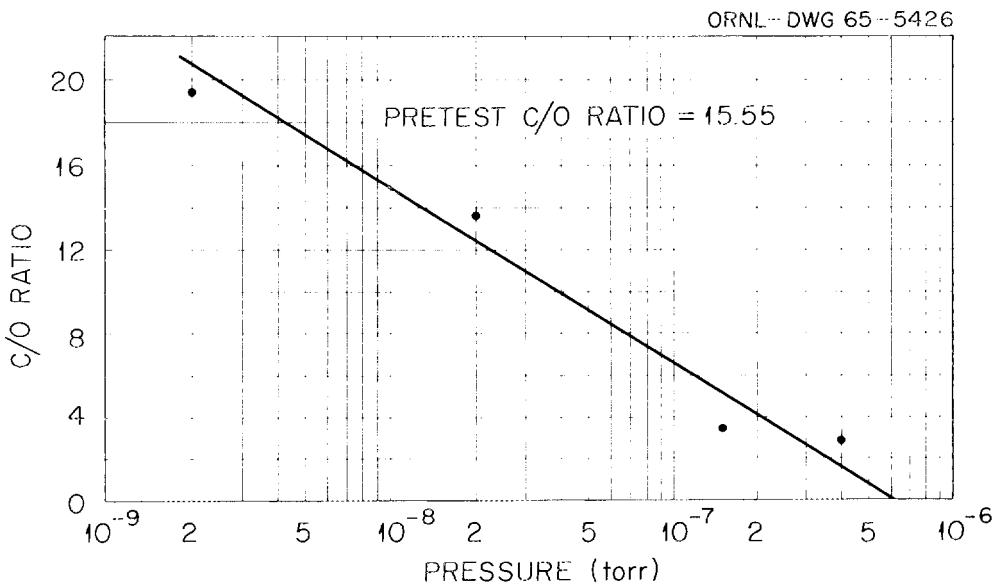

Fig. 14. The Variation of the Carbon-Oxygen Ratio of D-43 as a Function of the Test Pressure at 1500°C.

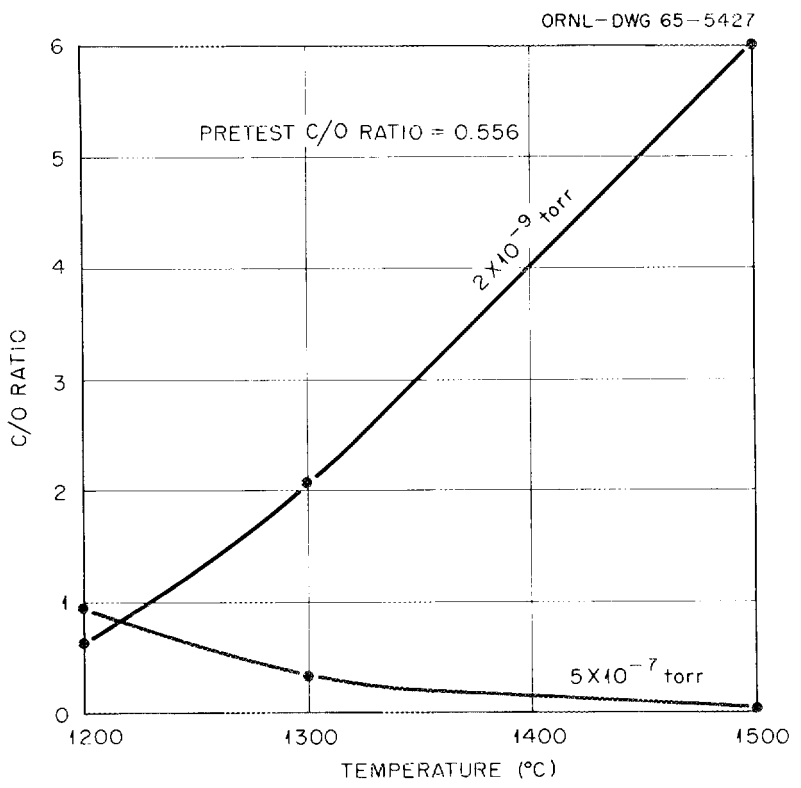

Fig. 15. The Variation of the Carbon-Oxygen Ratio of Nb-1% Zr as a Function of the Test Temperature at 10^{-9} and 10^{-7} torr.

the factors governing the reaction rate. Their results are summarized in Figs. 16 and 17. Figure 16 shows that the P_{CO} and P_{CO_2} resulting from the decarburization reactions decrease with the time of heat treatment even though the oxygen pressure increases. The decarburization rate under conditions where sufficient oxygen is available is governed by the diffusion rate of carbon in the alloy. Inasmuch as the diffusivity of carbon in tungsten increases with temperature,[20] the rate of CO generation should also increase with temperature, as shown in Fig. 17. In this example, the generation rate of CO approaches a saturation value at the higher temperature, since the rate is now governed by the pressure of oxygen — that is, by the rate of arrival of oxygen to the surface.

Sublimation

The phenomenon of sublimation results from the interaction of refractory alloys with oxidizing gases to form volatile oxides and is therefore a competitive reaction with the decarburization and the contamination processes. The process is complex because the amount and species of volatile oxides that are formed depend on the temperature and the oxidation pressure.

Figures 18, 19, and 20 identify the volatile oxide species formed by the reactions of oxygen with tungsten, molybdenum, and tantalum, respectively, over a wide range of temperatures.[21–23] In each example, the generation rate of a specific volatile oxide is seen to be temperature dependent and to pass characteristically through a maximum. The decrease in the reaction rates at temperatures above those at which

---

[20] I. I. Kovenskii, Diffusion in Body-Centered Cubic Metals, American Society for Metals, Metals Park, Ohio, 1964, p. 283.

[21] P. O. Schissel and O. C. Trulson, J. Chem. Phys. 43(2), 737–743 (July 1965).

[22] J. B. Berkowitz-Mattuck et al., J. Chem. Phys. 39(10), 2722–2730 (November 1963).

[23] J. Drowart et al., Mass Spectrometric Study of the Oxidation of Tungsten and Tantalum, Brussels University (Belgium), AD-622809 (August 1965).

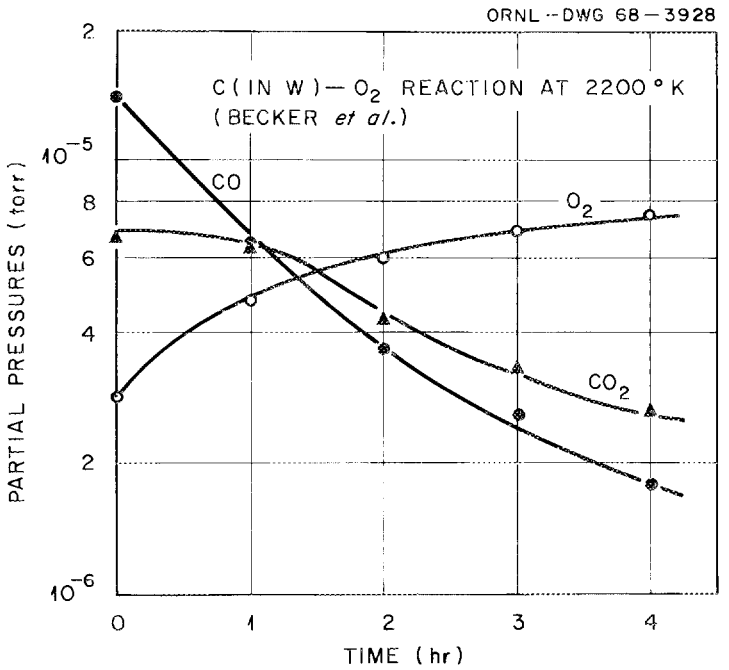

Fig. 16. Pressures of CO_2 and CO as a Function of Time Due to the Decarburization of Tungsten with Oxygen.

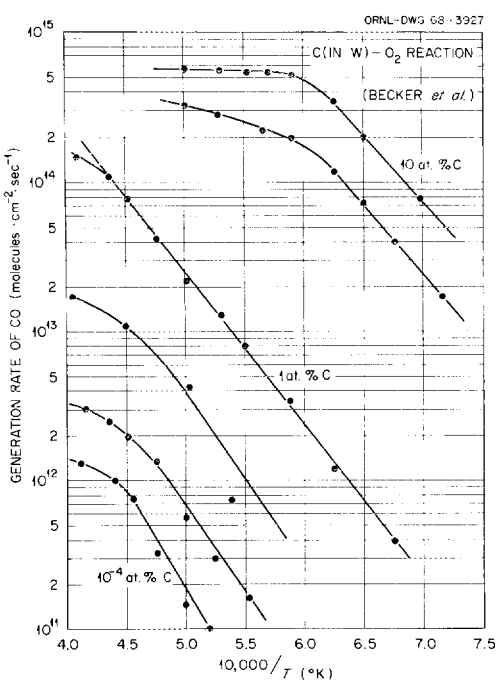

Fig. 17. Generation Rates of CO as a Function of 1/T Due to the Decarburization of Tungsten with Carbon.

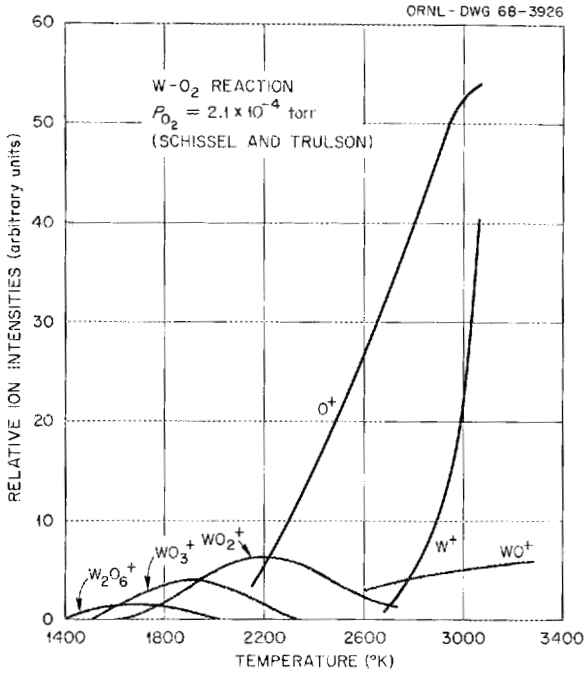

Fig. 18. Temperature Dependence of Ion Intensities: Tungsten-Oxygen Reaction.

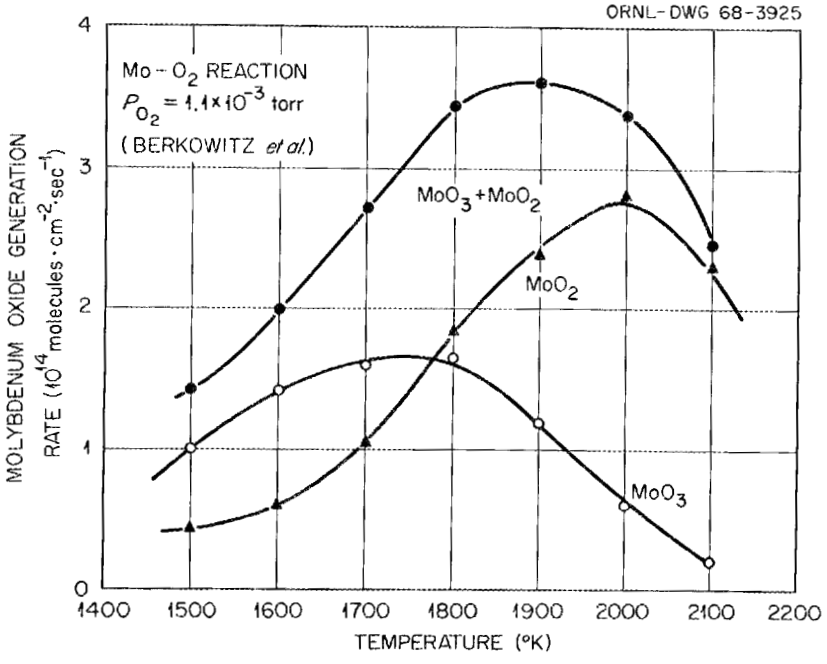

Fig. 19. Generation Rates of Volatile Molybdenum Oxides as a Function of Temperature During Sublimation of Molybdenum at 10^{-3} torr.

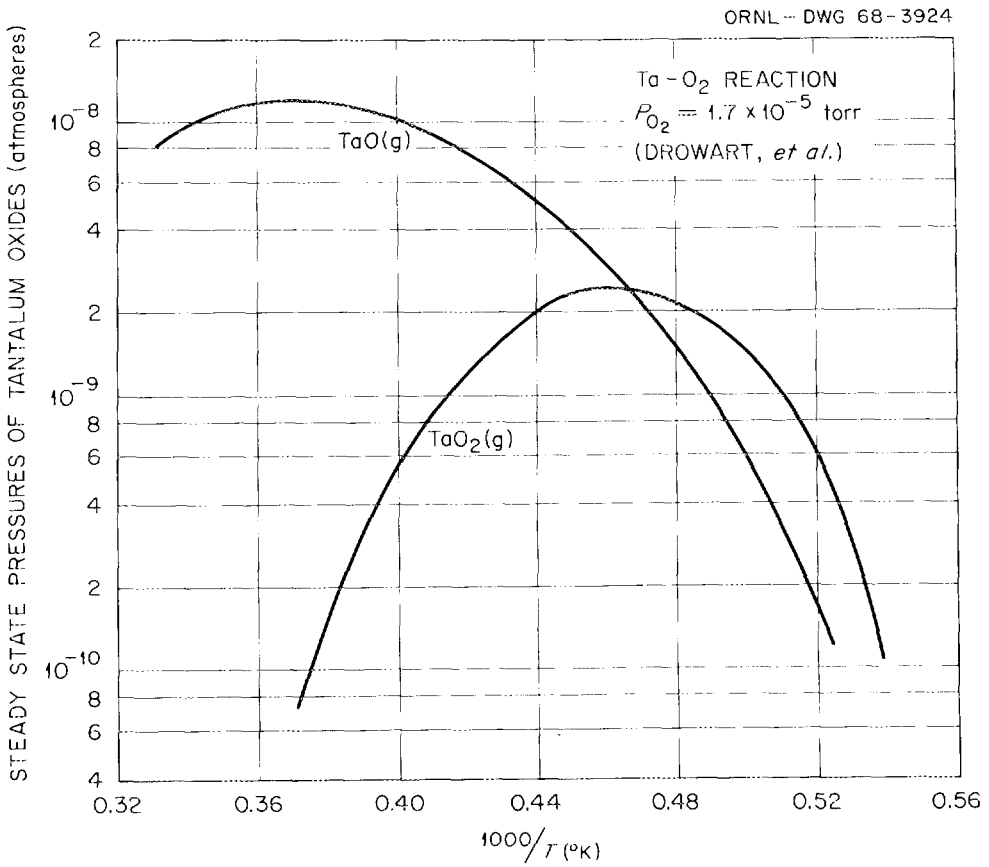

Fig. 20. Sublimation of Tantalum at 1.7×10^{-5} torr: Pressures of Volatile Tantalum Oxides as a Function of Temperature.

the maxima occur is attributed to a decrease in the number of adsorbed oxygen atoms at the surface. The temperature at which the maximum rate of sublimation occurs in molybdenum and tungsten increases with the oxygen pressure in the manner shown in Fig. 21. For a given pressure, note that molybdenum attains its maximum sublimation rate at a lower temperature than tungsten.

The sublimation rates of tungsten and molybdenum are constant at a given temperature and pressure — that is, the extent of the reaction increases linearly with time. In contrast, the sublimation rate of tantalum varies markedly with time.[24] Typical examples of the

[24] I. I. Kovenskii, Diffusion in Body-Centered Cubic Metals, American Society for Metals, Metals Park, Ohio, 1964, p. 283.

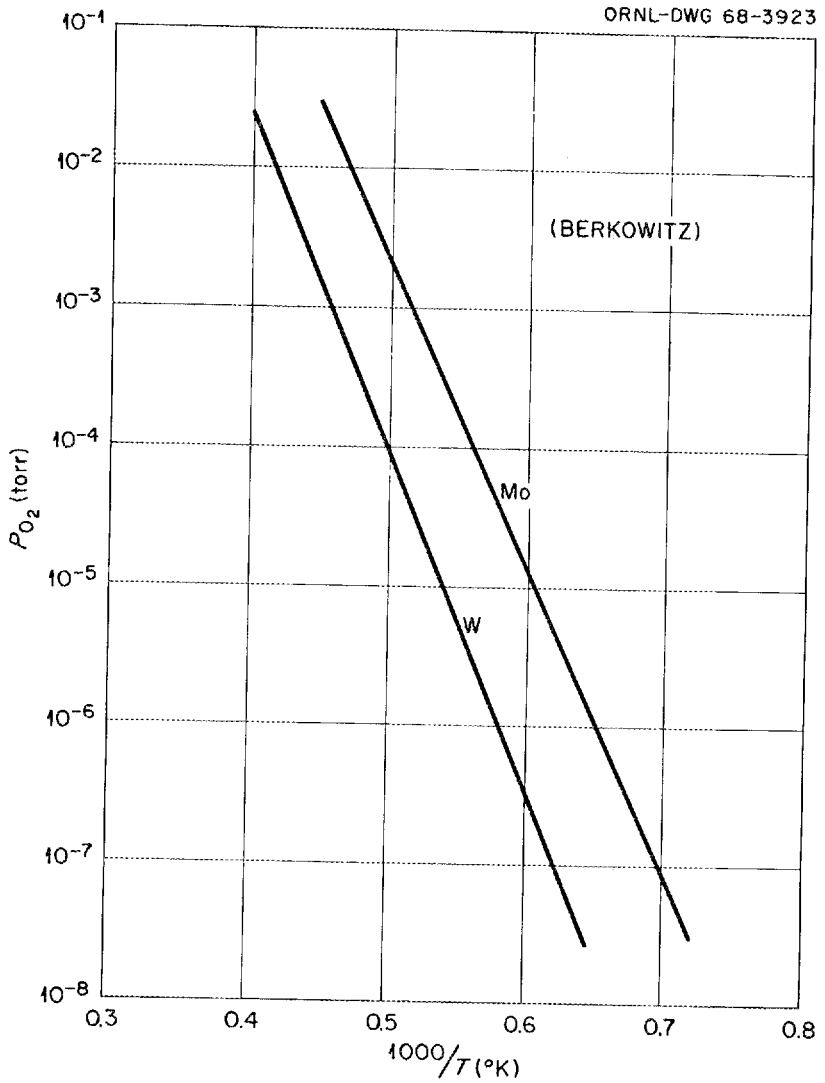

Fig. 21. Temperature-Pressure Relationship for Maximum Sublimation Rates of Tungsten and Molybdenum.

sublimation behavior are given in Fig. 22. In Fig. 22(a) the generation rate of TaO(g) increases continuously with the reaction time to a saturation value. This behavior results from the competition between the solution of oxygen in tantalum and the formation of a volatile oxide. When the oxygen pressure is increased as in Fig. 22(b), additional oxygen is taken into solution; and when saturation is reached, the sublimation rate again becomes constant. When the temperature is changed as in Fig. 22(c) and (d), a momentary change in the TaO intensities results from changes in the oxygen concentration on the surface

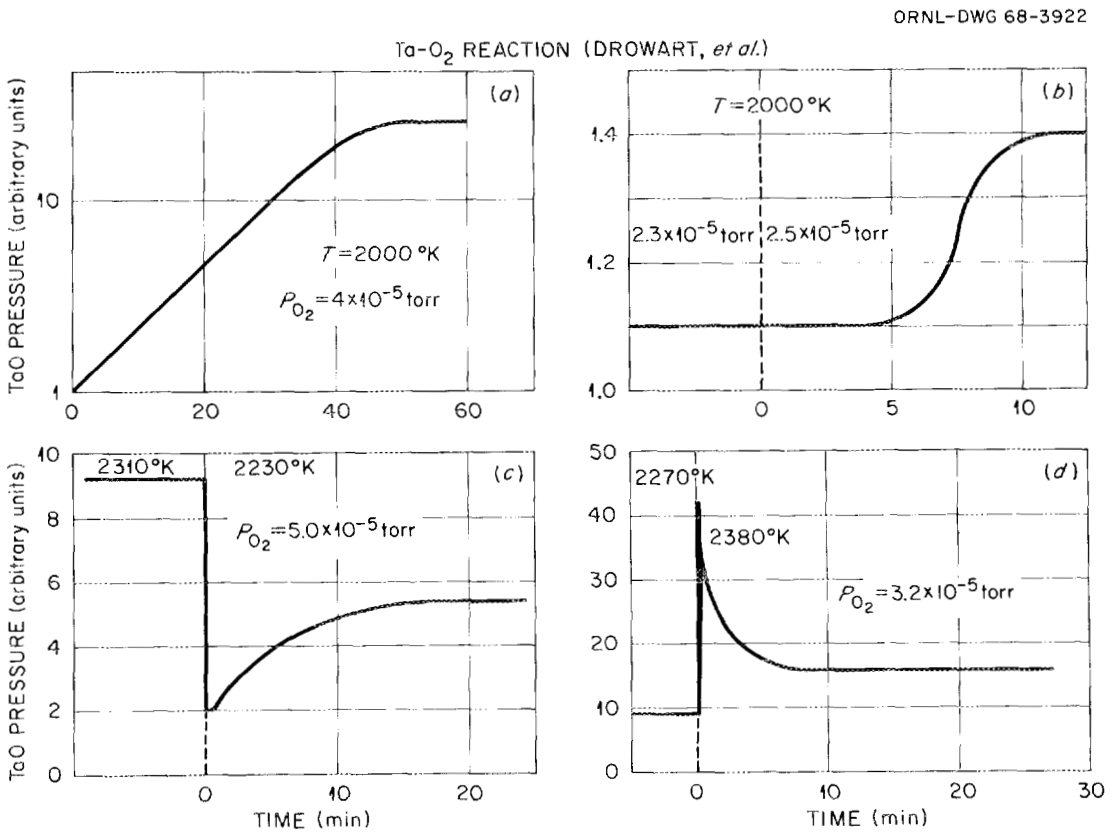

Fig. 22. Variation of the Pressure of TaO(g) with Time: (a) on First Exposure of Tantalum to Oxygen; (b) on Increasing Oxygen Pressure After Attainment of a Steady State; (c) on Lowering the Temperature After Attainment of a Steady State; and (d) on Increasing the Temperature After Attainment of a Steady State.

and in solution. The sublimation phenomenon is of minor consequence in terms of material losses in the normal course of heat treatment under ultrahigh vacuum conditions. But in a practical application in which the metal is exposed to an oxygen source such as an oxide fuel or other ceramic oxides, the saturation of the metal with oxygen and the sublimation process can, over an extended reaction time, be seen to be a potentially serious problem at very high temperatures.

Interaction of Refractory Metals in Inert Gases

Inert gas environments are being considered as the working media in advanced high-temperature power plants that use refractory metals. Inert gas environments are also a logical substitute for vacuum

environments. Unfortunately, the lack of sufficient data precludes a detailed characterization of the interactions similar to that presented in the previous sections. From some available data, it appears that the parameters that govern the interactions of refractory metals with the impurities in vacua also apply in the case of the inert gases (see Table 2). Some differences do exist, however, and are discussed qualitatively below.

A major disadvantage of the use of an inert gas is the great difficulty of measuring precisely the concentrations of the active impurity gases. For example, if the decarburization of D-43 is to be prevented during annealing at 1500°C in 1 atm pressure of inert gas, the permissible pressure of active gases according to Fig. 14 is 1×10^{-8} torr. This concentration in the inert gas is approximately 10^{-11} atm or 10^{-5} ppm. It is readily apparent that impurity concentration in this range cannot be detected easily.

Excluding the technological difficulty of impurity gas analysis, there is an advantage in the use of inert gases. According to theory their presence will lower the reaction rate between the refractory alloys and the active gas impurities since the impurity gases collide with and must diffuse through the inert gases to reach the alloy surface — that is, the incident rate for a given pressure of an active gas at the alloy surface is lower in an inert gas than in a vacuum.

Table 6 compares the reaction rates of niobium and tantalum in helium, in argon, and in vacua. Due to the difficulty of analysis, the impurity contents of the inert gases for the examples given are unknown at the test temperatures. By comparing the reaction rates in the various environments, we can see that these inert gas environments correspond to vacua in the range between 10^{-5} to 10^{-7} torr. Since 1×10^{-3} torr is about 1 ppm, the effective impurity gas pressures in the argon tests are calculated to be between 10^{-2} to 10^{-4} ppm. Because inert gases are not usually this pure, we concluded that the incident rates of the active gases are lowered by the inert gas.

Table 6. Comparison of the Contamination Rates of Niobium and Tantalum in Helium, Argon and Vacua

Test Temperature (°C)	Test Material	Exposure (hr)	Environment	Reaction Rate (mg cm^{-2} sec^{-1})
982	Nb	2538	Static argon	8×10^{-5} [a]
1010	Nb	56	Static argon	1×10^{-2} [a]
1150	Nb and Ta	500	300 psi He, high velocity	4×10^{-3} [b]
1000	Nb	5	$P_{O_2} = 1 \times 10^{-5}$ torr	1×10^{-2} [c]
1000	Nb and Ta	1000	Vacuum, $P = 2 \times 10^{-7}$ torr	5×10^{-5} [d]

[a]H. E. McCoy and D. A. Douglas, "Effect of Various Gaseous Contaminants on the Strength and Formability of Columbium," pp. 85–118 in Columbium Metallurgy, ed. by D. L. Douglass and F. W. Kunz, Interscience, New York, 1961.

[b]L. A. Charlot et al., Corrosion of Superalloys and Refractory Metals in High Temperature Flowing Helium, BNWL-SA-1137 (March 1967).

[c]H. Inouye, "The Oxidation of Columbium at Low Oxygen Pressures," pp. 649–665 in Columbium Metallurgy, ed. by D. L. Douglass and F. W. Kunz, Interscience, New York, 1961.

[d]H. Inouye, "The Contamination of Refractory Metals in Vacua Below 10^{-6} Torr," pp. 871–883 in Refractory Metals and Alloys III: Applied Aspects, Vol 30, ed. by Robert I. Jaffee, Gordon & Breach Science Publishers, New York, 1966.

Controlling Gas-Metal Reactions

A gaseous environment that is in equilibrium with the interstitials in the refractory alloy at the heat-treating conditions is probably an unattainable goal. Since many of the parameters that control the reaction kinetics are now known, however, some practical methods can be employed to suppress many of the undesirable reactions.

First is the geometry variable and its influence on the extent of the reaction. Experimental data conclusively confirmed that the extent of contamination was proportional to the surface-to-volume ratio and inversely proportional to the thickness. Thus, if it is known that non-equilibrium conditions prevail, the surface-to-volume ratio of the refractory alloy should be held to a minimum and its thickness to a maximum.

Secondly, the heat-treating conditions should be chosen, if possible, to minimize the degree of equilibrium disparity. To do this it would be necessary to have gas-metal equilibrium data and the interstitial analysis of the alloy. Data for most alloys do not exist; however, it is pointed out that maxima in the reaction rates occur at intermediate temperatures. Therefore, these temperatures are not desirable.

Further reductions in the interactions of active gases with refractory alloys are possible through the use of protective foil wraps on refractory metals. Metals that are the most reactive toward the active gases would appear to be the suitable choice. As an example, Table 4 suggests that the preferred foil materials should contain the more reactive elements, such as titanium, zirconium, and hafnium, so that they will react preferentially with the noxious gases.

Figure 23 compares the effects of molybdenum, tantalum, and Nb–1% Zr envelopes on the extent of contamination of Nb–1% Zr at 2.7×10^{-7} torr for 1000 hr (ref. 25). These data show that foil wraps markedly reduce the extent of contamination; note, however, that their efficiency with respect to minimizing the extent of contamination was in the order molybdenum, tantalum, then Nb–1% Zr, which is the reverse of the order of their reactivity according to Table 6. Further evaluation of this technique showed that the effectiveness of protective envelopes was independent of the foil composition but dependent on the extent of the leaks in the seams of the envelope. Therefore, the function of a foil wrap is not to getter the active gases but to serve as a physical barrier to the incident noxious gases. This concept of protective foils necessarily requires that the sticking probability must be low as was shown to be the case in an earlier section.

The dominant presence of carbon monoxide in the heat-treating environment, the prevalence of oxygen contamination, and the observed phenomenon of decarburization above 1200°C and 1×10^{-8} torr (see Figs. 14 and 15) indicate that the oxidizing gases are the most

---

[25]H. Inouye, "The Contamination of Refractory Metals in Vacua Below 10^{-6} Torr," pp. 871–883 in Refractory Metals and Alloys III: Applied Aspects, Vol 30, ed. by Robert I. Jaffee, Gordon & Breach Science Publishers, New York, 1966.

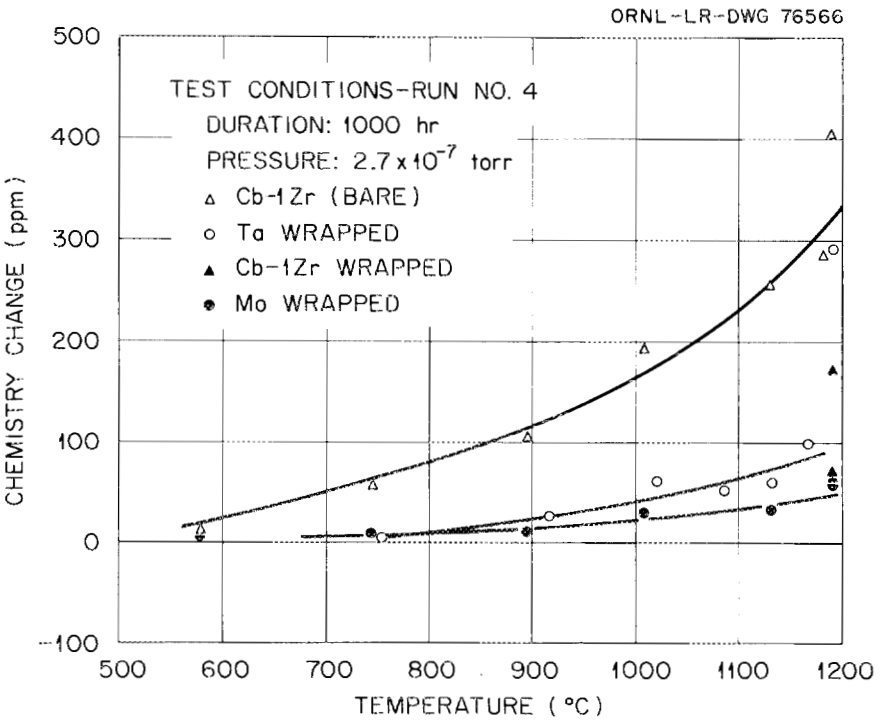

Fig. 23. Influence of Foil Wraps on Reducing the Contamination of Nb–1% Zr at 2.7×10^{-7} torr.

aggressive active gases with respect to the refractory alloys. Perkins and Lytton[26] were successful in preventing decarburization or restoring the carbon content of molybdenum alloys during annealing by introducing low-pressure CH_4 into the vacuum environment. On the other hand, CH_4 has been used to reduce the extent of oxygen contamination of TZM (ref. 25) as shown in Fig. 24. These data show that CH_4 at 6×10^{-7} torr was capable of lowering the extent of the oxygen contamination at a base pressure of 2×10^{-7} torr by a factor of approximately 3 at 1200°C but was not effective in preventing decarburization of the alloy.

Summary and Conclusions

A review of the published data shows that the interactions of refractory alloys based on niobium, tantalum, molybdenum, and tungsten

[26]R. A. Perkins and J. L. Lytton, Effect of Processing Variables on the Structure and Properties of Refractory Metals, Part I, AFML-TR-65-234 (July 1965).

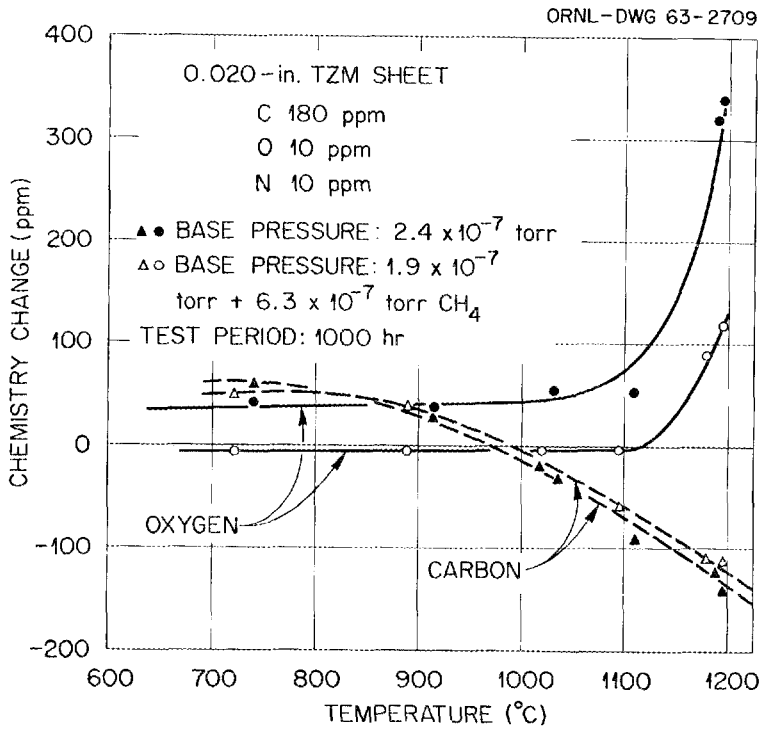

Fig. 24. Effect of CH_4 on the Oxygen Contamination of TZM.

with the active gases in vacua and inert gas environments can be grouped into processes that result in contamination, degassing, decarburization, and sublimation of the refractory alloy as volatile oxides. From 600 to 2000°C these reactions occur in the pressure range between 10^{-3} and 10^{-10} torr without the formation of a surface reaction product. The extent and kinetics of these reactions are governed precisely by the degree of equilibrium disparity — that is, the deviation of the interstitial concentration of the alloy from the concentration the alloy would have when equilibrium is obtained at a given temperature and pressure.

For the contamination process, the reaction rate is given by $Q_a = \alpha Q_i$, where α is the sticking probability and Q_i is the incident rate of the gas at the alloy surface. In general, less than 10% of the incident gas reacts with refractory alloys at high temperatures — that is, α has a maximum value of approximately 0.10. Since the reaction proceeds toward equilibrium, α initially is a maximum for a given temperature and pressure but decreases as equilibrium is approached in

accordance with the empirical relationship $\alpha = \alpha_o (1 - C_m/C_e)$, where α_o is the sticking probability for an interstitial free alloy and C_m and C_e are the mean and equilibrium interstitial content, respectively. The effects of pressure, temperature, reaction time, and alloying components on the reaction kinetics are explained in terms of this relationship.

A decarburization process results from an oxidation reaction that produces carbon monoxide as the reaction product and is encountered above 1200°C and approximately 10^{-8} torr. The decarburization rate is proportional to the diffusion rate of carbon in the alloy at the low temperatures and in the presence of sufficient amounts of oxygen, but at high temperatures is dependent on the oxygen pressure.

Sublimation of refractory alloys as volatile oxides results from their interaction with oxidizing gases at the higher temperatures and is a competitive reaction with the decarburization and contamination processes. The reaction rates increase with pressure but characteristically go through maxima for a given pressure as the temperature is increased. For each metal-oxygen reaction, several volatile oxide species are formed.

The contamination rates of refractory alloys by the active gases in helium and argon are equivalent to the rates observed in vacua in the range 10^{-5} to 10^{-7} torr. It appears from the experimental data available that inert gases significantly lower the incident rate of the active gas at the alloy surface, as predicted by theory.

The principles governing the reaction kinetics suggest that the extent of the several reactions can be reduced by minimizing the surface-to-volume ratio and selecting heat-treating conditions to minimize the degree of equilibrium disparity. Other techniques that have been successful are the use of protective foil envelopes and the use of low-pressure CH_4 to neutralize the oxidizing gases.

ORNL-4312
UC-25 – Metals, Ceramics, and Materials

INTERNAL DISTRIBUTION

1–3. Central Research Library
4–5. ORNL – Y-12 Technical Library
Document Reference Section
6–25. Laboratory Records Department
26. Laboratory Records, ORNL RC
27. ORNL Patent Office
28. C. F. Baes
29. C. R. Baldock
30. R. J. Beaver
31. D. S. Billington
32. C. M. Blood
33. E. G. Bohlmann
34. D. T. Bourgette
35. G. E. Boyd
36. E. J. Breeding
37. W. E. Browning, Jr.
38. T. A. Butler
39. A. K. Chakraborty
40. E. L. Compere
41. G. L. Copeland
42. G. E. Creek
43. C. W. Cunningham
44. J. E. Cunningham
45. J. R. DiStefano
46. R. G. Donnelly
47. D. S. Easton
48. J. E. Epperson
49. K. Farrell
50. J. I. Federer
51. B. Fleischer
52. M. Fontana
53. H. A. Friedman
54. J. H Frye, Jr.
55. R. E. Gehlbach
56. P. A. Gnadt
57. T. G. Godfrey
58. J. L. Gregg
59. Karl W. Haff
60. W. O. Harms
61–63. M. R. Hill
64. D. O. Hobson
65. H. F. Holmes
66–69. H. Inouye
70. W. W. Johnston, Jr.
71. G. W. Keilholtz
72. R. L. Klueh
73. J. W. Koger
74. C. E. Larson
75. R. J. Lauer
76. J. M. Leitnaker
77. T. B. Lindemer
78. K. H. Lin
79. B. T. Loh
80. R. A. Lorenz
81. A. P. Litman
82. H. G. MacPherson
83. H. E. McCoy
84. D. L. McElroy
85. J. P. Moore
86. F. H. Neill
87. T. M. Nilsson
88. J. C. Ogle
89. A. R. Olsen
90. M. F. Osborne
91. L. R. Phillips
92. A. C. Schaffhauser
93. S. T. Sekula
94. R. L. Senn
95. C. E. Sessions
96. W. A. Sibley
97. K. Spear
98. P. H. Spindler
99. R. L. Stephenson
100. J. O. Stiegler
101. D. A. Sundberg
102. V. J. Tennery
103–147. D. B. Trauger
148. S. C. Weaver
149. A. M. Weinberg
150. F. W. Wiffen
151. R. K. Williams
152. A. Wolfenden
153. J. P. Young
154. C. M. Adams, Jr. (consultant)
155. Leo Brewer (consultant)
156. L. S. Darken (consultant)
157. J. A. Krumhansl (consultant)

EXTERNAL DISTRIBUTION

158. Dan Albreds, University of California, Berkeley, Calif.
159. Benjamin C. Allen, Battelle Memorial Institute, Columbus, Ohio
160. G. M. Anderson, AEC, Washington
161. C. H. Armbruster, Wright-Patterson AFB
162. V. P. Calkins, General Electric, NMPO
163. S. S. Christopher, AEC, Washington
164. D. F. Cope, RDT, SSR, AEC, Oak Ridge Operations
165. J.W.R. Creagh, NASA, Lewis Research Center
166. J. Davis, Jet Propulsion Laboratory
167. R. W. Dayton, Battelle Memorial Institute, Columbus, Ohio
168. G. K. Dicker, AEC, Washington
169. E. M. Douthett, AEC, Washington
170. D. DeHalas, Pacific Northwest Laboratory, Richland
171. J. K. Elbaum, Code MAMP, Wright-Patterson AFB
172. N. B. Elsner, Gulf General Atomic
173. P. N. Flagella, General Electric, NMPO, Cincinnati
174. D. C. Goldberg, Westinghouse Astronuclear Laboratory
175. D. H. Gurinsky, Brookhaven National Laboratory
176. R. Hall, NASA, Lewis Research Center
177. R. C. Hamilton, Institute for Defense Analyses, 1666 Connecticut Avenue, N.W., Washington, D. C.
178. E. E. Hoffman, Nuclear Systems Programs—MSD, General Electric, Cincinnati
179. J. R. Holland, Division 9322, Sandia Laboratories, Albuquerque, New Mexico 87115
180. W. R. Holman, Lawrence Radiation Laboratory
181. F. J. Huegel, University of California, Berkeley, Calif.
182. C. Johnson, Space Nuclear Systems Division, Space Electric Power Office, AEC, Washington, D. C. 20545
183. J. S. Kane, University of California, Berkeley, Calif.
184. Don Keller, Battelle Memorial Institute, Columbus, Ohio
185. W. J. Larkin, AEC, Oak Ridge Operations
186. P. J. Levine, Westinghouse Advanced Reactors Division, Waltz Mill Site, Box 158, Madison, Pa. 15663
187. J. J. Lombardo, NASA, Lewis Research Center
188. J. J. Lynch, NASA, Washington
189. C. L. Matthews, RDT, OSR, AEC, Oak Ridge National Laboratory
190. T. P. Moffitt, NASA, Lewis Research Center
191. T. A. Moss, NASA, Lewis Research Center
192. R. A. Noland, Argonne National Laboratory
193. F. G. Ostermann, Wright-Patterson AFB
194. W. E. Ray, Westinghouse Advanced Reactors Division, Waltz Mill Site, Box 158, Madison, Pa. 15663
195. T. K. Roche, Union Carbide Corporation, Materials Systems Division, Kokomo
196. Louis Rosenblum, NASA, Lewis Research Center
197. A. J. Rothman, Lawrence Radiation Laboratory
198. A. L. Rothman, University of California, Berkeley, Calif.

199. B. Rubin, Lawrence Radiation Laboratory
200. N. D. Sanders, NASA, Lewis Research Center
201. H. Schwartz, NASA, Lewis Research Center
202. F. C. Schwenk, AEC, Washington
203. S. C. Srivastava, Department of Material Science, State University of New York, Stony Brook, New York 11790
204. P. G. Shewmon, Argonne National Laboratory
205. J. M. Simmons, AEC, Washington
206. H. T. Sumison, NASA, Ames Research, Moffett Field, Calif. 94035
207. D. K. Stevens, AEC, Washington
208. J. A. Swartout, Union Carbide Corporation, New York
209. G. W. Wensch, AEC, Washington
210. G. A. Whitlow, Westinghouse Advanced Reactors Division, Waltz Mill Site, Box 158, Madison, Pa. 15663
211. M. J. Whitman, AEC, Washington
212. W. R. Witzke, NASA, Lewis Research Center
213. Laboratory and University Division, AEC, ORO
214-410. Given distribution as shown in TID-4500 under Metals, Ceramics, and Materials category